行政院國家科學委員會補助專題研究計畫成果報告

※※※※※※※※※※※※※※※※※※※※※※※※※※※※※※
※ 　　　　　　　　　　　　　　　　　　　　　　　　　　　　※
※ 　　　　　　　　　　　　　　　　　　　　　　　　　　　　※
※ **酵素型 WO_3-IrO_2 二極體陣列葡萄糖感測元件之速率研究** ※
※ 　　　　　　　　　　　　　　　　　　　　　　　　　　　　※
※ 　　　　　　　　　　　　　　　　　　　　　　　　　　　　※
※※※※※※※※※※※※※※※※※※※※※※※※※※※※※※

計 畫 類 別 ： 個 別 型 計 畫

計 畫 編 號 ： NSC90-2215-E-009-060

執 行 期 限 ： 90 **年** 8 **月** 1 **日**－91 **年** 10 **月** 31 **日**

計 畫 主 持 人 ： 趙 書 琦

本成果報告包括以下應繳交之附件：

- □赴國外出差或研習，心得報告一份
- □赴大陸地區出差或研習，心得報告一份
- □出席國際學術會議心得報告及發表之論文各一份
- □國際合作研究計畫國外研究報告書一份

執 行 單 位 ： 國立交通大學電子物理系

中 華 民 國 ： 　　91 **年** 10 **月** 26 **日**

行 政 院 國 家 科 學 委 員 會 專 題 研 究 計 畫 成 果 報 告

酵素型 WO_3-IrO_2 二極體陣列葡萄糖感測元件之速率研究

Dynamic switching rate in enzymatic WO_3 - IrO_2 diode array microsensors for glucose

計畫編號：NSC90-2215-E-009-060
執行期限：90 年 8 月 1 日－91 年 10 月 31 日
主持人：趙書琦　　計畫助理[17)]
國立交通大學電子物理系

一、中文摘要

以 WO_3 - IrO_2 之類材料組成的食物新鮮度感測器，會因為二極體陣列所使用之 Pt 電極間距較大，而形成很大的 RC 時間延遲，造成元件的感測切換反應速率遲緩。本計畫係以一種溝渠影蔭鍍膜技術，製作出具有次微米間距之 Pt 電極陣列，大幅降低元件的 RC 時間延遲，有效的提昇了元件的反應速率，使其邁入更實用化的境界。

關鍵詞：溝渠影蔭鍍膜、反應速率、二極體、微感測器、新鮮、WO_3、IrO_2

Abstract

In food freshness microsensors built from WO_3 - IrO_2, slow electrical signals can arise due to large inter-electrode gaps in the Pt array. Particularly, the RC-time delay associated with these large gaps will severely limit the device's switching rate. Through a newly developed Pt patterning technique termed "trench-shadow deposition," the inter-electrode gap has been reduced to ~0.4 μm. These submicron gaps can diminish the RC-time delay, achieving enhancement of the device's switching rate to that of a few seconds.

Keywords ： Trench-shadow Deposition, Switching Rate, Diode, Microsensor, Freshness, WO_3, IrO_2

二、緣由與目的

This investigation calls for the enhancement of the dynamic switching rate in the present device through reducing the inter-electrode gap in the Pt array. Due to their exceptional stability, insertion oxides (such as WO_3, IrO_2 and $Ni(OH)_2$) have attracted wide research interests. Unfortunately, in the case of food freshness microsensors built from insertion oxides, past incorporation of large gaps between Pt electrodes (~200-400 μm) introduced large resistance and capacitance components in the device. This RC-time delay has significantly limited the device's switching rate:

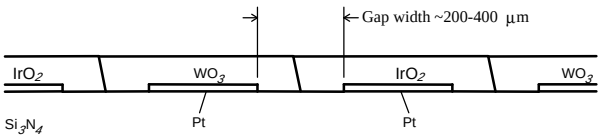

(1)

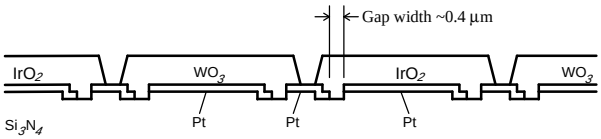

(2)

To alleviate the problem, we propose to replace the previously used Pt array with a new design, (2), featuring submicron gaps (~0.4 μm). As shown in (2), we also placed WO_3 and IrO_2 in indirect contact via a bridging Pt electrode. This measure will avoid difficulties in the alignment of the WO_3 and IrO_2 films within a ~0.4 μm-wide gap.

The present investigation is an expansion on the previous microsensor diode that is usable in resolving glucose concentration gradient in food materials. It is constructed of single diodes that are operable in liquids at room temperature, Fig. 3. The previous diode device is based on pH-sensitive WO_3 and IrO_2, which interact with H^+ in the reversible redox reactions,[1,2)]

$$WO_3 \text{ (bleached)} + xH^+ + xe^- \leftrightarrow H_xWO_3 \text{ (colored), and} \quad (3)$$

$$IrO_2\cdot(H_2O) \text{ (colored)} + H^+ + e^- \leftrightarrow Ir(OH)_3 \text{ (bleached).} \quad (4)$$

Both WO_3 and IrO_2 reductions to the conducting H_xWO_3 and insulating $Ir(OH)_3$ occur at more positive electrochemical

potentials in acidic media over a range of pH values between ~2-12[3,4] (reactions (3) and (4)). These redox transformations arise due to the insertion of ionic species into the oxides, which can produce large conductance changes.[4,5] The present work is inspired by the earlier discoveries in this laboratory that a bicarbonate (HCO_3^-)-doped, polyvinyl alcohol (PVA) solid polymer matrix interfaced with WO_3 or IrO_2, can respond to CO_2 in terms of resistance or potential across closely spaced microelectrodes at 1 atm and room temperature.[6,11] Despite the advantages of such relatively simple chemical-sensitive resistors and potentiometers, practical use is less attractive due to the lack of a built-in current "turn-on" capacity commonly found in diode and transistor-based microsensors.[7] However, WO_3 and IrO_2 are known to be complementary cathodic and anodic electrochromic materials,[8] and have been used to demonstrate optical attenuation. By connecting WO_3 and IrO_2 in series, as shown in Fig. 3, both oxides become conducting under positive bias in the forward direction and insulating under negative bias in the reverse direction. However, the device function cannot be fully explained by treating the oxides simply as variable series resistors. Since H_xWO_3/WO_3 is cathodically electroactive whereas $Ir(OH)_3/IrO_2$ is anodically electroactive, the transport of charge across the WO_3/IrO_2 interface is allowed only in the forward direction and forbidden in the opposite direction. The current growth in the forward direction can occur readily via the thermodynamically favored reduction of IrO_2 by the reduced H_xWO_3. In fact, the attenuation of current in the reverse direction is more an indication that the oxidation of $Ir(OH)_3$ by the oxidized WO_3 is thermodynamically infeasible.

For this reason, rectification in $-WO_3-IrO_2-$, (1), should not be affected as we opt for $-WO_3-Pt-IrO_2-$, (2), since it is governed by thermodynamic free energies. As reported previously,[9] our experiments show exactly that. The WO_3 and IrO_2 films, when contacted via a third Pt electrode in between can still be used to generate the same rectification as before. The results also show that geometrical areas involved in the direct overlap of WO_3 and IrO_2 affect the magnitude of the current, but the overall rectification is not changed.

In our view, this type of rectification governed by thermodynamic free energies is the major advantage for constructing such diodes based on the contact of WO_3 and IrO_2. The devices will be durable since they are made of robust materials. Unlike previous microsensors based on conventional or organic diodes,[7,10] their electrical functions in gases and liquids are not susceptible to the environmental variabilities arising from interfacial or material instability. Previous exploratory experiments in this area have led to our results[11] that the electrical contacts of solid WO_3 and IrO_2 films, sputtered on adjacent Pt electrodes and covered by the polymer blend PVA·$KHCO_3$, can be used to generate diodelike current-voltage outputs that respond to CO_2 gas. We have later reported similar devices that are operable in aqueous solutions. When devices based on the contact of sputtered WO_3 and IrO_2 are covered by a glucose oxidase-containing polymer, they can exhibit reversible and reproducible glucose-dependent, diodelike current rectification in liquids at room temperature. A surface modification scheme employing the bi-layer Ta_2O_5/Al_2O_3 membrane coated over the WO_3 - IrO_2 array to eliminate redox species interference was investigated last year. We now report a new device, a submicron-gap microsensor diode array based on the serially connected contacts of sputtered WO_3 and IrO_2 via Pt, Figs. 3, 5 and 9.

三、實驗方法

The Pt-pad electrodes in Fig. 3 can no longer be fabricated by use of the lift-off procedure described earlier.[6] “Lift-off” requires a relatively thick photoresist. From our past experiments, resolution worsening due to thick photoresist limits the inter-electrode separation to > 4 μm. Since Pt is a robust material that forms essentially ohmic contacts with WO_3 and IrO_2,[9] it is deemed irreplaceable. The patterning problem involving Pt is solved by employing a technique we have termed “trench-shadow deposition.” First, trenches are cut into Si_3N_4 using reactive-ion etching. The Pt deposition is then carried out at an oblique angle, utilizing the well-formed steps generated in the trenches as shadow masks, Fig. 4. This technique has been used to yield Pt arrays separated by submicron gaps ~0.4 μm wide, as illustrated in Fig. 5. The dimensions of Pt electrode themselves are typically 200-300 μm wide and 3,000 μm long.

To avoid annealing the IrO_2 due to

heating by subsequent WO_3 deposition, sputtering of the WO_3 target (99.99%, Pure Tech) at radiofrequency is carried out first under 20% O_2 in Ar at a total pressure of 90 mTorr, in the same apparatus as used before.[9] A stainless-steel sheet with laser-opened holes or a Si wafer with micromachined V-grooves is used as the deposition mask. The mask and devices on the wafer are pressed onto a heated substrate platen at 676 K.[3] The deposited WO_3 films exhibit broad cyclic voltammograms in aqueous 1.0 M $HClO_4$ over the potential range of 0.3 to -0.3 V vs. a saturated calomel electrode, as reported previously.[3] Characterization of the films on indium-tin oxide glass shows electrochromism in the visible region and a wide range of absorption change under potential cycling in aqueous 1.0 M H_2SO_4. The change is ~15-85% in transmittance at 650 nm, near the wavelength of maximum difference in the absorption band. The process for derivatizing the Pt electrodes with the amorphous IrO_2 film, next to the WO_3 films (Fig. 3), by the reactive sputtering method and the characterizations have been described earlier.[9]

The deposition of Ta_2O_5 and Al_2O_3 membranes (~200-300 Å thick) is carried out by sputtering of a Ta_2O_5 or Al_2O_3 target (99.99%, Pure Tech) under 45% O_2 in Ar at a total pressure of 100 mTorr, in the same apparatus as used before. The integrity of the sputtered Ta_2O_5 or Al_2O_3 membrane as a barrier to electron transport from solution redox species is tested on a flat Pt electrode. Potential cycling of the Pt/Ta_2O_5 or Pt/Al_2O_3 electrode in aqueous 10 mM $K_3Fe(CN)_6$ in 0.10 M KCl electrolyte has yielded no discernible cyclic voltammetric waves that are characteristic of the redox species even at the highest current sensitivity of the potentiostat (BAS CV-50W, Bioanalytical Systems). The prepared WO_3, IrO_2 Ta_2O_5 and Al_2O_3 films are robust and adhere strongly to the Pt surface. No difficulty such as peeling has been encountered throughout the course of our experiment. After deposition of the oxide films, electrical contact of individual Pt electrodes is made using Ag epoxy, which is later encapsulated using insulating epoxy. Optical microscopy reveals that uniform bleaching and coloring can occur in each of the insertion oxide films on Pt. As shown in Fig. 3, each film has most of its lower surface in contact with the underlying Pt electrode. This forces the potential drop to be confined only to the WO_3 and IrO_2 within the two submicron gaps across the Pt/WO_3/Pt/IrO_2/Pt interfaces, leaving the individual films on Pt approximately at equipotential and of the same color.

In the next step, the whole device active area is covered with covalently immobilized glucose oxidase (GOD, Type VII from *Aspergillus niger*, Sigma) (Fig. 3). This enzyme layer is used for creating a glucose-modulated pH environment specifically for the diode. The procedure for the covalent immobilization of GOD is performed separately in two sequential steps:[12,13]

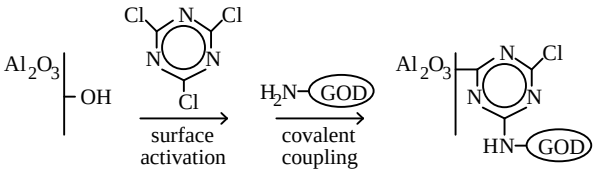

(5)

The first step involves the activation of the exposed Al_2O_3 surface (Fig. 3) by cyanuric chloride. The reason for the choice is due to the simplicity of the cyanuric chloride reaction over the other reagents. The second step involves the preparation of immobilized enzyme derivatives via covalent coupling in the presence of glucose.[12,13] In order to protect the active site, it is common practice to carry out this reaction in the presence of the substrate. The reaction also needs to be performed under mild conditions. Low temperature, low ionic strength and pH in the physiological range are important factors in preventing the enzyme from denaturing. The determination of the optimal conditions for the maximum retention of enzyme activity is a trial-and-error process. Before activation, the exposed Al_2O_3 surface is pretreated in aqueous 0.1 M KOH for 60 s to grow hydroxyl groups. After washing with deionized H_2O and dried, the surface is reacted with 0.05 M cyanuric chloride in benzene for 2 h at 50°C. Before covalent coupling, GOD (1,200 units or 10 mg) is dissolved in 0.2 ml aqueous 0.1 M phosphate solution (pH 8.0) saturated with glucose. No other supporting electrolyte has been added since the enzyme layer functions only as a source or sink for H^+, and not as an electrolyte to carry ionic current. The enzyme solution (100 μl) is placed with a microsyringe over the exposed active area of

the diode array (Fig. 3) and chilled at 4ºC for 12 h to form the non-leaching glucose oxidase enzyme layer. This covalently immobilized enzyme layer forms light-yellow films that are highly adhesive to Al_2O_3. No peeling of the films has been encountered throughout the electrical experiments. Enzyme layers immobilized with the same procedure separately on glass slides have been immersed in H_2O at 37ºC for at least 4 months without any visible sign of disintegration.

The switching current of the submicron-gap microsensor diode, reaching equilibrium as a function of time in Fig. 1, has been measured by use of a Keithley 236 source-measure unit, Fig. 3. The glucose solution flows are generated by switching between the streams of two digital peristaltic pumps (Rainin Dynamax RP-1). Aqueous 0.01 M phosphate buffer (pH 7.0) is used as the carrier solution in both streams but only one contains 0.2 mM glucose. The glucose injection experiment in Fig. 2 is performed on a flow-injection apparatus. This FIA includes a combination of one syringe pump and one peristaltic pump.[14] The diode arrays packaged into integral flow cells are used, as earlier,[14] to allow exposure to glucose solutions with different concentrations. The conditions of glucose concentrations carried in the buffer solutions are generated by proportioning the flowrate of microprocessor-controlled infusion pumps (Sage 341B). Low concentration aqueous phosphate (0.01 M, pH 7.0) buffer solution is always used as the carrier for glucose to facilitate pH change in immobilized GOD.

Bovine meat samples are first incubated at 37ºC for 24-48 h in air to induce depletion of glucose by microorganisms at the surface. A vertical incision is made to half the sample, which is then carefully laid onto the microsensor with the incised surface pressed against the array, Fig. 9.

四、結果與討論

Experiments show that reducing the inter-electrode gap to ~0.4 μm has largely enhanced the dynamic switching rate of the device. In Fig. 1, when a current switching experiment for the submicron-gap microsensor diode is performed, the device under test shows a fast response toward glucose concentration. The equilibration time is ~5 s, which is faster than before by a factor of ~10^2. This result has also enabled us to run glucose flow-injection experiments for the first time on the microsensors built from WO_3 and IrO_2, Fig. 2. The fast current transients induced by glucose injections have a pulse rise-time on the order of ~1 s. Finally, we have improved the switching rate of our device to fully comply with the specification set by the sensor industry.

Experiments also show that neither reducing the inter-electrode gap to ~0.4 μm nor adding the bridging Pt electrode, Fig. 3, has affected the rectification of WO_3 - IrO_2. Fig. 6 shows the glucose-dependent current-voltage characteristics of 1 single submicron-gap diode within an array of 5 diodes based on WO_3 and IrO_2. The glucose creates a pH-regulated environment for the diodes (Fig. 3), through its pH-lowering effect, as previously reported.[15] Glucose equilibration catalyzed by the immobilized glucose oxidase proceeds according to the reaction

$$\text{Glucose} + 1/2O_2 \xrightarrow{\text{GOD}} \text{Gluconate}^- + H^+. \quad (6)$$

As results of the glucose-dependent experiment in Fig. 6 show, diodes based on WO_3 and IrO_2 undergo a current decrease in the forward direction when the glucose concentration is increased within the range of 0.2-10 mM in phosphate buffer solutions. This result is consistent with the WO_3 and IrO_2 redox processes (reactions (3) and (4)). The electrochemical potentials in both reactions become more positive in more acidic environments. This shift can be considered to result from the pH-dependent changes in the potential drop across the Helmholtz layer at the surface of both oxides, as stated earlier.[6,9] On the potential scale, the shifting of redox potentials towards the positive region renders reductions more favorable than oxidations under fixed driving force. When the bias voltage is unchanged, the current passing through a less fully oxidized IrO_2 in series with a more fully reduced H_xWO_3 in the forward direction still shows a loss due to the current-limiting effect exerted by the higher resistance (Fig. 6). The fact that the experimentally determined pH sensitivity for our IrO_2 (~58 mV/ΔpH) in aqueous solutions,[9] is higher than that for our WO_3 (~52 to 54 mV/ΔpH), is relevant and should be noted. This means that up to ~5 mV/ΔpH positive displacement of IrO_2 potential in excess of that of WO_3 can be expected in the more acidic diode

environments created by glucose. That should further contribute to the current loss in the forward direction. The current loss in Fig. 6 in the forward direction is also confirmed by the observed progressive coloration in H_xWO_3 and discoloration in IrO_2 as the pH is lowered in the immobilized GOD layer by glucose solution under a fixed positive bias.

The new submicron-gap diodes are markedly durable and reproducible. Repeated voltage sweeps under each glucose concentration in Fig. 6 give almost identical current-voltage signals. Neither the rectification behavior nor the current amplitudes show signs of degradation. Figure 5 shows the layout and the diode numbering scheme of the new array. Under a fixed 1.6 V bias, switching the solution between 0.2 to 10 mM glucose in phosphate buffer turns the new diodes in the 5-diode array to the "on" and "off" states (Fig. 7). They exhibit ~-(8 to 18) mA and 0 mA current change in the forward direction, respectively (Fig. 8). The current switchings are reversible and reproducible and can be carried out for all diodes on the array without significant deterioration for >48 h.

The sensitivity or dynamic range of the submicron-gap diodes on the array for glucose concentration is found to be dependent on the pH value of the carrier buffer solution used. Glucose is capable of inducing a larger pH drop in immobilized GOD layer when the buffer solution is more basic. As shown in Fig. 8, the submicron-gap diodes have a valid range for glucose concentrations between ~0.2-10 mM. Separate experiments show that the diodes can actually respond to glucose from 60 to 0.01 mM with acceptable signal-to-noise ratio. It has also been determined that the glucose-induced current change in the forward direction is proportional to the logarithm of the glucose concentration to which immobilized GOD is exposed, as shown in the inset in Fig. 8.

Next, experiments are performed to demonstrate that the new diode array is capable of resolving the 1-dimensional spatial distribution of glucose concentration in food material. A bovine tissue incubated for bacterial growth at the surface (controlled at 37ºC in air for 24 h) is placed over the array, Fig. 9. The diodes on the array, each biased individually, show spatially resolved rectifying I-V characteristics, Fig. 10. The detected forward currents at 1.6 V bias in Fig. 10 produce a 1-dimensional, 5-point plot of the blood glucose distribution that has been generated by the surface-to-bulk bacterial consumption near the tissue surface. Since glucose is progressively depleted from the surface as a function of time, this result can be used to build a quantitative database on the sensing of freshness[16] in food materials. In particular, the new linear diode array has a potential for practical use as a microsensor for acquiring the “freshness plots” of foods in several seconds.

This work reveals that oxide-based microsensors are durable and that, in principle, many oxides with widely varying properties can be used to fabricate sensing devices with special electrical characteristics. In addition, functions can be readily built-in to enhance the switching rate. Work is already under way, in this laboratory, to incorporate this diode function in some other microsensors.

五、計畫成果自評

本研究內容與原計畫相符程度約95%**。達成預期目標，包括創新元件之發現、其理論之推導和模式建立、所用實驗原型和系統之建立、以及人才培育等。本研究成果具有學術、應用價值，可發表於國外期刊和申請專利。本研究主要發現，包括以獨具的整流機制，建構感測用二極體元件，並以溝渠影蔭鍍膜技術，製作關鍵的次微米間距電極陣列，賦予元件快速反應的特質。以這種元件為基礎，可以發展出其他二極體的陣列微感測器，能用於各種生物液體中，獲得生物分子的空間分佈資訊，並向感測資訊快速化邁進。這是應用傳統二極體建立微感測器無法做到的。**

六、參考文獻

1) M. O. Schloh, N. Leventis and M. S. Wrighton: J. Appl. Phys. **66** (1989) 965.
2) B. Scrosati: *Applications of Electroactive Polymers*, ed. B. Scrosati (Chapman & Hall, London, 1993) p. 256.
3) M. J. Natan, T. E. Mallouk and M. S. Wrighton: J. Phys. Chem. **91** (1987) 648.
4) K. Paztor, A. Sekiguchi, N. Shimo, N. Kitamura and H. Masuhara: Sens. & Actuat. B **12** (1993) 231.
5) M. J. Natan and M. S. Wrighton: Prog. Inorg. Chem. **37** (1989) 391.
6) S. Chao: Jpn. J. Appl. Phys. **32** (1993) L1346.
7) J. W. Gardner: *Microsensors, Principles and Applications* (John Wiley, Chichester,

1994) p. 235.
8) R. D. Rauh and S. F. Cogan: J. Electrochem. Soc. **140** (1993) 378.
9) S. Chao: Jpn. J. Appl. Phys., Part 2, **37** (1998) 245.
10) N. Leventis, M. O. Schloh, M. J. Natan, J. J. Hickman and M. S. Wrighton: Chem. Mater. **2** (1990) 568.
11) J. C. Lue and S. Chao: Jpn. J. Appl. Phys. **36** (1997) 2292.
12) P. W. Carr and L. D. Bowers: *Immobilized Enzymes in Analytical and Clinical Chemistry* (J. Wiley & Sons, New York, 1980).
13) B. Eggins: *Biosensors* (Wiley Teubner, Chichester, 1996) p. 37.
14) S. Chao: Meas. Sci. Technol. **7** (1996) 737.
15) Y. Hanazato, M. Nakako and S. Shiono: IEEE Trans. Electron Devices **33** (1986) 47.
16) Sensor Review, **9** (1989) 15.
17) **莊益林**

七、圖表

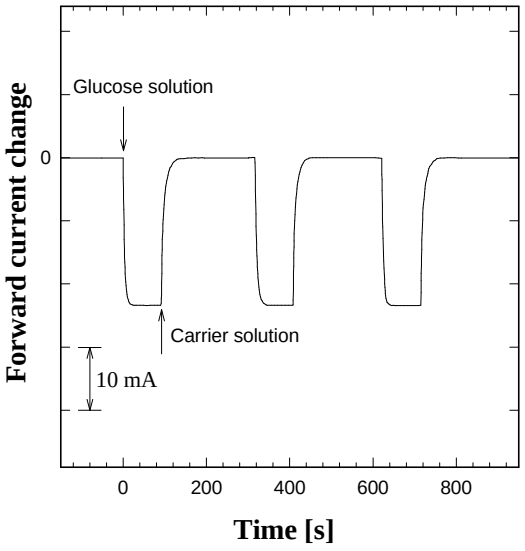

Fig. 1. A current switching experiment for the submicron-gap microsensor diode, showing fast on-off response (equilibration time ~5 s) induced by glucose solution flows (0.2 mM). The forward bias was 1.6 V and the flow conditions were produced by switching between the streams of two peristaltic pumps.[14)]

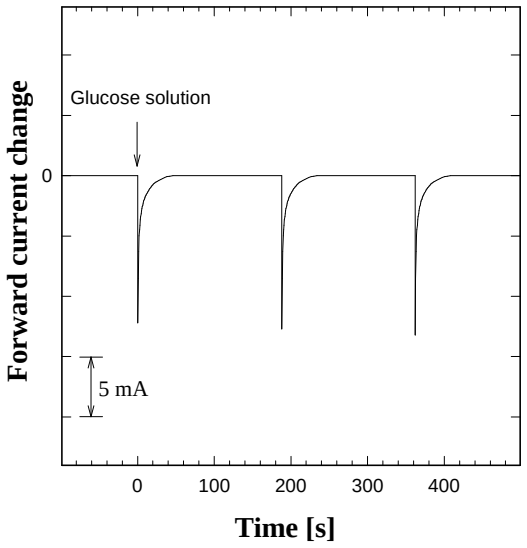

Fig. 2. A flow-injection experiment for the submicron-gap microsensor diode, showing fast current transients (pulse rise-time ~1 s) induced by repeated glucose injections (0.3 ml, 0.2 mM).

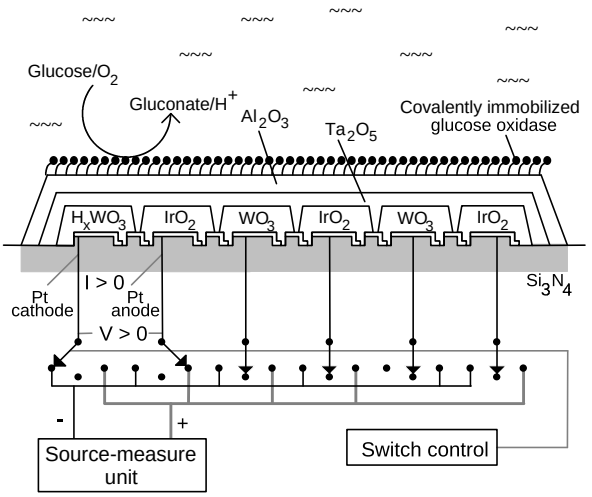

Fig. 3. Scheme showing the new submicron-gap microsensor diodes under test, with one forward-biased enzymatic diode based on the contact of WO_3 and IrO_2 on Si in the array under glucose modulation in H_2O.

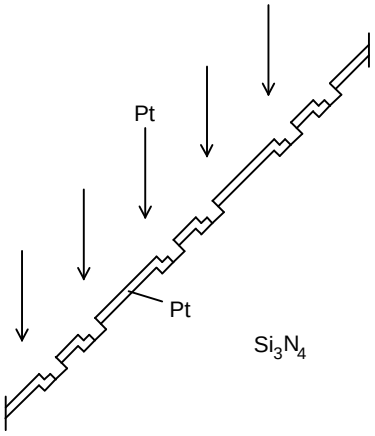

Fig. 4. The “trench-shadowing” method for the deposition of Pt generating electrode arrays with sub-micron gaps.

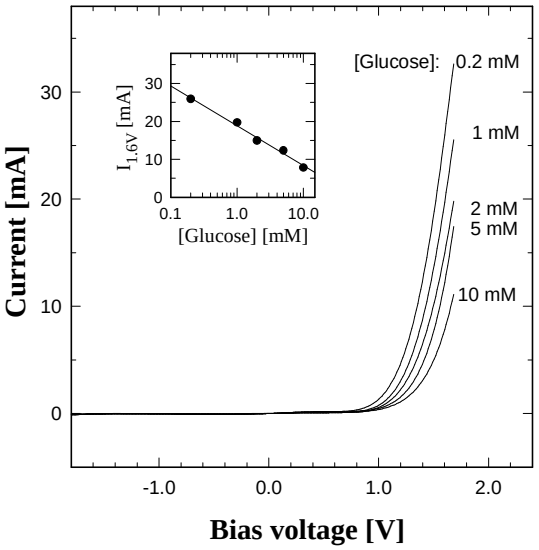

Fig. 6. Typical single diode current-voltage characteristics in a 5-diode submicron-gap microsensor array (Fig. 3) under the modulation of glucose concentrations in phosphate buffer at 298 K.

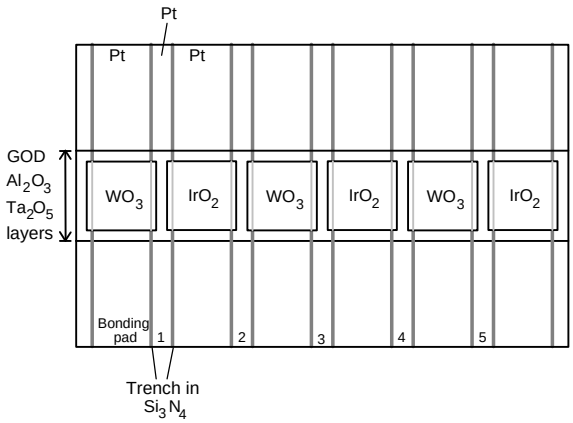

Fig. 5. Typical layout and numbering scheme of Pt electrodes and the diode array based on the contact of WO_3 and IrO_2 on Si.

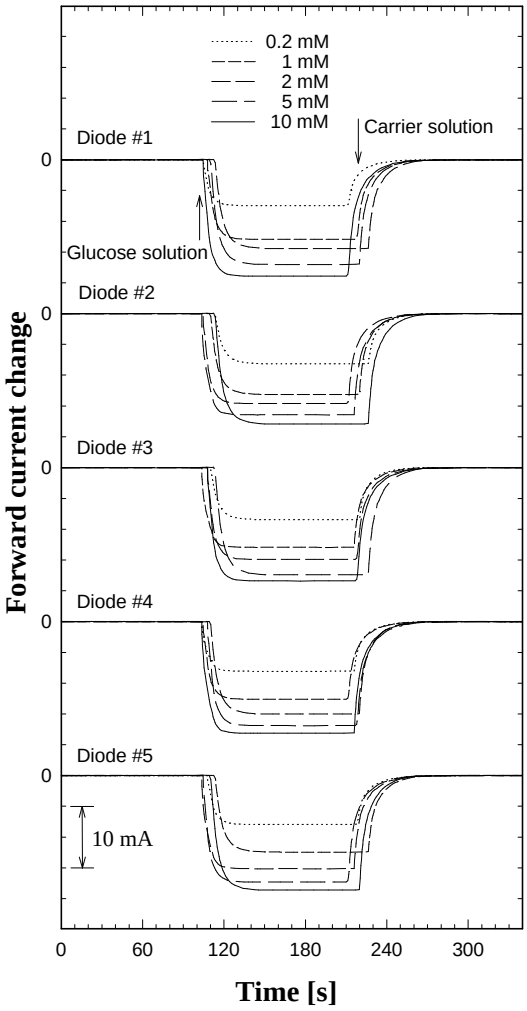

Fig. 7. Typical electrical response of a 5-diode, submicron-gap microsensor array. The glucose concentration-induced switching behaviors of each diode are produced under a forward bias of 1.6 V at 298 K. The carrier flows are 10 mM aqueous phosphate buffer solution adjusted to pH 7.0.

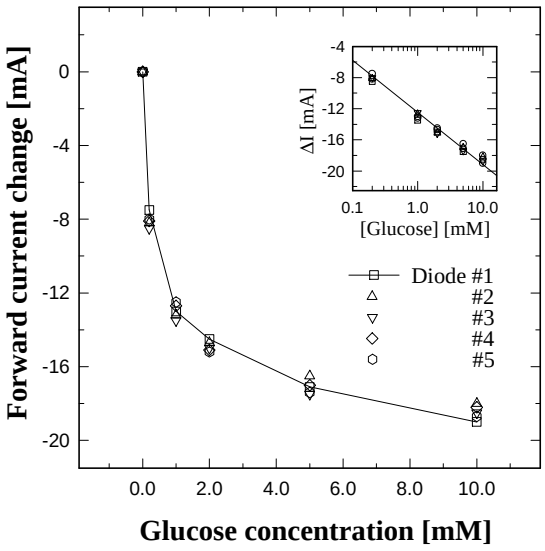

Fig. 8. Typical current changes in the forward direction (1.6 V bias) of a 5-diode, submicron-gap microsensor array induced by glucose concentrations in phosphate buffer at pH 7.0 and 298 K.

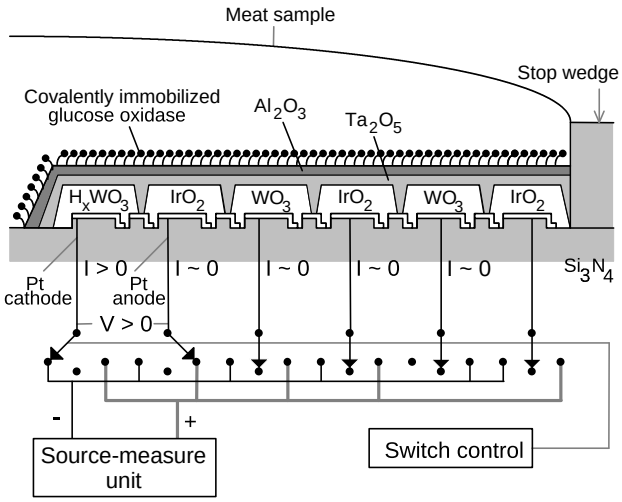

Fig. 9. The sub-micron gap enzymatic diode array, one forward-biased diode based on the contact of WO_3 and IrO_2 on Si, and the incubated meat sample measurement scheme.

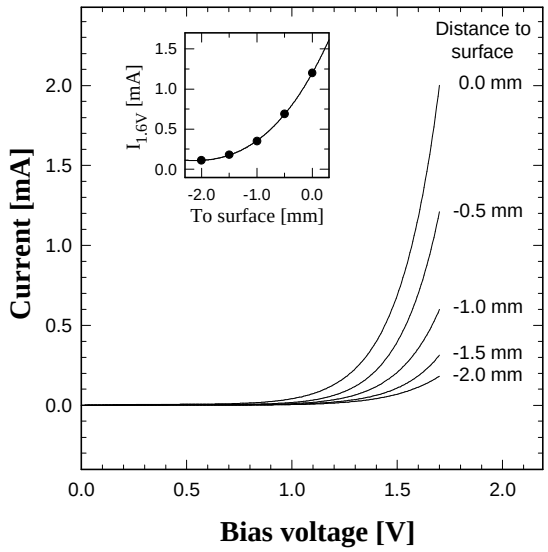

Fig. 10. Typical spatially resolved current in the forward direction (1.6 V bias) of a 5-diode, submicron-gap microsensor array induced by the glucose concentration gradient in an incubated meat sample at 298 K in uncontrolled air atmosphere. (Diodes are labeled by their distance to the incubation surface, Fig. 9).